Applied Ocean Research 48 (2014) 1–9

Contents lists available at ScienceDirect

Applied Ocean Research

journal homepage: www.elsevier.com/locate/apor

Dynamic analysis of coupling between floating top-end heave and riser's vortex-induced vibration by using finite element simulations

Weimin Chen [a,*], Min Li [b], Shuangxi Guo [a], Kuan Gan [b]

[a] Key Laboratory for Mechanics in Fluid Solid Coupling System, Institute of Mechanics, Chinese Academy of Sciences, Beijing 100190, China
[b] School of Aeronautics Science and Technology, Beijing University of Aeronautics and Astronautics, Beijing 100191, China

ARTICLE INFO

Article history:
Received 5 March 2014
Received in revised form 16 May 2014
Accepted 9 July 2014
Available online 9 August 2014

Keywords:
Heave
Parameter excitation
Vortex-induced vibration
Slender riser

ABSTRACT

The dynamic coupling between floating top and submarine riser becomes more remarkable owing to larger fluctuation amplitude of floating platform in deeper water, compared to fixed platform in shallow water. In this study, the impacts of top-end vertical motion (heave) on riser's vortex-induced vibration (VIV) are explored by means of finite element simulations. A coupled hydrodynamic force approach, regarding vortex-induced lift force along with fluid drag force, is developed, which takes into account of the interaction between instantaneous structure motion and fluid dynamics. Then the dynamic responses of the integrate system including both floating top-end and a riser undergoing VIV are examined based on our numerical simulations. The influences of platform heave, in terms of heave frequencies and tension ratios, on riser's VIV are presented. Our numerical results show that the dynamic response displacement of riser becomes several times larger than the displacement for the case without top-end motion. The impact of top heave on riser's VIV gets larger as the modal order number drops. Moreover, an interesting phenomenon, called the mode transition, is observed particularly at lower vibration frequencies due to the natural dynamic characteristics of the slender riser. We suggest that, in practices of riser design, a combined excitation needs to be considered for the accurate dynamic analysis of slender marine structures subjected to a top-end motion and VIV.

1. Introduction

With the development of oil and gas exploration toward deeper ocean, more deepwater platforms such as spar, tension leg and semi-submersible platforms have been put into services. Marine risers are usually employed to convey gas and oil, or optical and electrical information, between top-end vessel and sea bed. Consequently, the vortex-induced vibration (VIV) of slender risers with large aspect ratio becomes more complicated as water depth increases. For example, the shedding modes or frequencies of wake-vortex may vary along the riser length (or depending on water depth) rather than keeping just constant. Additionally, the dynamic characteristics of slender riser usually offers lower-frequency and higher-density natural modes owing to its larger structure flexibility. Therefore, the VIV of a slender riser frequently presents some new phenomena, such as multi-mode VIV, traveling wave and wide-band random vibration [1–3], which have presented new challenges to researchers of ocean engineering.

On the other hand, compared with the fixed platform in shallow water, the floating platform in deep water has larger motion amplitude, and the coupling between top-end vessel and submarine riser appears to be more pronounced. Moreover, new problems such as additional lock-in region, parametric excitation and nonlinear response due to the coupling are introduced [4,5]. It is noted that the tension fluctuation of top-end heave may cause riser's VIV involving higher-order modes along with larger-amplitude dynamic response, e.g. 10% and 20–100% higher displacement and shear stress respectively than the case without top-end motion [5]. Moreover, Silveira [6] found the mode jump during the dynamic response of a slender riser and Park and Jung [7] reported that the parametric excitation (caused by top-end heave) alters the response pattern of a long slender marine structure. Their results demonstrated that a combined excitation needs to be considered for the accurate dynamic analysis of long slender marine structures subjected to a surface vessel motion.

Among the researches on the dynamic coupling between top-end vessel and marine riser, most of them mainly addressed on dynamic response of top-end itself. Generally, the methods used to analyze the dynamic responses can be classified into two kinds: quasi-static method [8–11] and coupled method [12–17]. In quasi-static method, flexible riser is modeled as a spring with lumped mass, and only the hydrostatic restoring force exerted upon top-end vessel by riser is considered. Spanos [10] used a horizontal spring to model the riser and lumped the top-end as a mass to study

* Corresponding author. Tel.: +86 010 82543891; fax: +86 10 82338527.
E-mail address: wmchen@imech.ac.cn (W. Chen).

0141-1187/$ – see front matter © 2014 Elsevier Ltd. All rights reserved.
http://dx.doi.org/10.1016/j.apor.2014.07.005

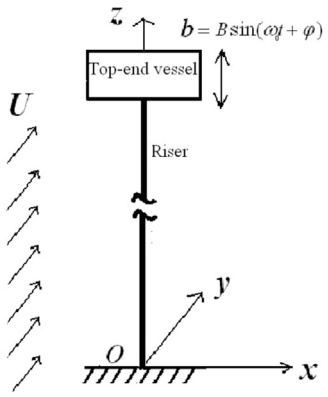

a The platform-riser system and the flow distribution

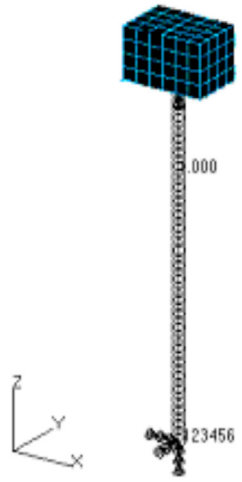

b The finite element model of the platform-riser system

Fig. 1. The platform-riser system sketch. (a) The platform-riser system and the flow distribution. (b) The finite element model of the platform-riser system.

effect of riser's stiffness on dynamic response of a SPAR. Ormberg [8], Kim [9] and Wichers [11] studied the interaction between floating vessel and mooring system and compared quasi-static method with coupled method. Their results indicated that the static methods may give an underestimation of load endurance of mooring system.

In coupled method, submarine riser and its hydrodynamic force exerted by ambient ocean current or wave are mostly simplified [16,18,19], e.g. the Morison formula is employed to model hydrodynamic force. Lee [18] used a linear tensional string to simulate tension leg and analyzed the leg dynamic response while the top-end vessel experiences a periodical surge. His results showed that there was a leg vibration mode similar with the platform while the vibration amplitude changes with wave period. Tahara [19] employed the empirical formula of the Young's modulus suggested by Bosman [12] to examine the mooring system response of a SPAR undergoing heave. By comparing his result with that of a linearly elastic mooring system, he found a remarkable difference between the two results. Park [7] implemented a numerical analysis of lateral responses of a long slender marine structure under combined parametric and forcing excitations. Tang [20] used the Van der Pol oscillator to model VIV and studied multi-mode vibration during parametric excitations. Their results demonstrated that a combined excitation would give greater amplitude than that of VIV or heave alone.

In addition, it is worthwhile to mention that the mechanisms of dynamic coupling, between top vessel and submarine riser, due

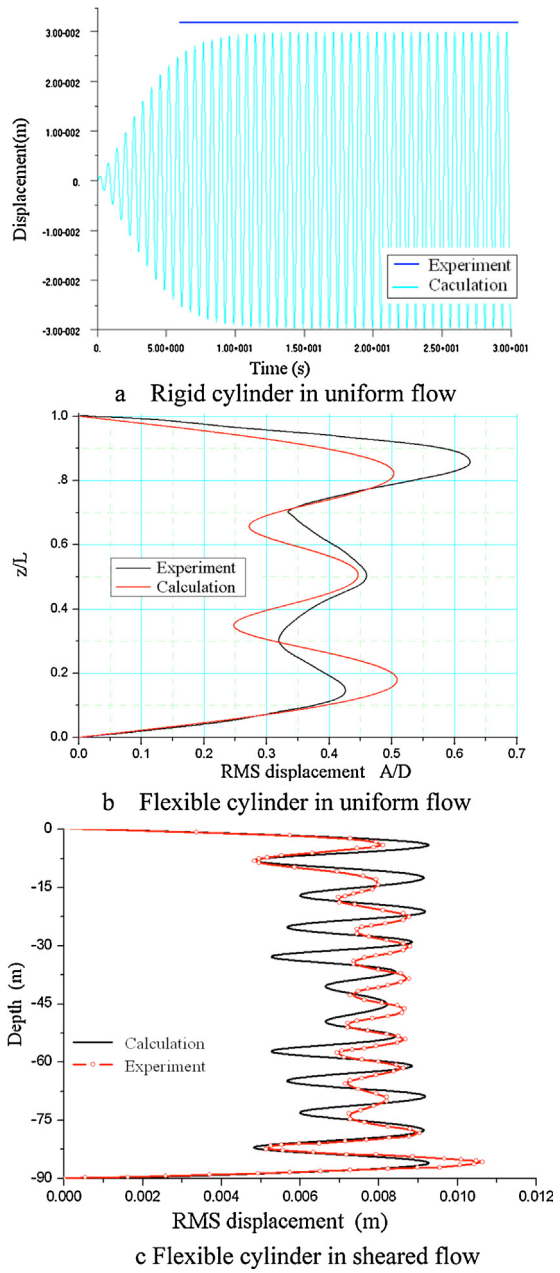

Fig. 2. Comparisons of VIV response between the presented numerical simulation and the existing experimental results of (a) rigid cylinder in uniform flow; (b) flexible cylinder in uniform flow; and (c) flexible cylinder in sheared flow.

to different vessel motions are quite different. Taking horizontal motion of vessel, i.e. sway or surge, as an example, the transverse vibration of top-end propagates along riser. This transverse vibration may directly interact with riser's VIV. Even, the vibrating boundary condition introduced by top-end motion might cause nonlinearly couplings such as response amplification and new lock-in. However, if top-end heave is considered, it introduces not only a moving boundary to riser's dynamics but, more essentially, a fluctuating tension of riser. This time-varying tension in fact offers a periodically varying structural property, thus, the consequence may be parametric excitation of riser [21–24]. When it comes to parametric excitation, most previous studies addressed on stability region of a time-varying system, e.g. the theoretical solutions of stability region based on different theories [21,23,25,26] or the dynamic response of an Euler beam with simplified hydrodynamic force model [27,28]. Moreover, riser's lateral motion due to ocean

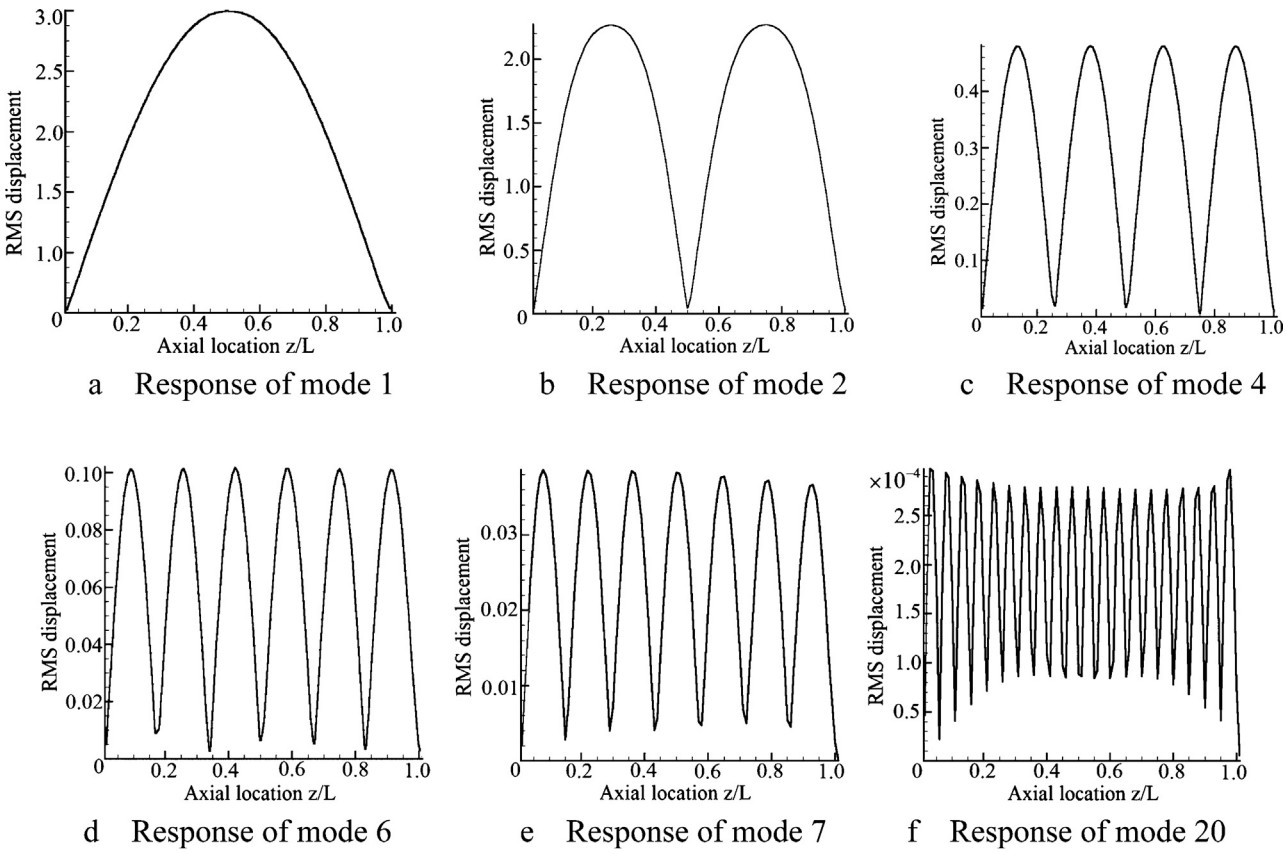

Fig. 3. RMS displacements of dynamic response of the riser experiencing both top-end heave and VIV. (a) Response of mode 1. (b) Response of mode 2. (c) Response of mode 4. (d) Response of mode 6. (e) Response of mode 7. (f) Response of mode 20.

current or wave, rather than vortex-induce force in the wake filed of riser (riser's VIV), were mainly considered.

In this paper, the dynamic interaction between top-end vessel heave and riser's VIV is investigated. First, we develop a hydrodynamic approach to model the vortex-induced lift force which, in essence, depends on simultaneous structure motion. Then the dynamic response of the integrate system including top-end vessel heave and riser VIV are examined by means of finite element simulations. Effects of top-end heave frequencies along with tension ratios on riser's dynamic response and vibration propagation are examined so as to have a deeper insight into the interaction between top-end vessel heave and riser VIV.

2. Coupled model of the system including top-end heave and riser's VIV

2.1. Dynamic behavior of a riser parametrically excited due to top-end heave

Essentially, top-end vessel heave introduces a time-varying structural property, a fluctuating tension of riser. This periodically varying structural property consequently causes parametric excitation of riser. Here, we would first have a theoretical analysis of the dynamic behavior of such a riser, modeled as an Euler beam pinned at two ends. The governing equation of the Euler beam is

$$EI\frac{\partial^4 x(z,t)}{\partial z^4} - (T_0 + T\cos\omega_0 t)\frac{\partial^2 x(z,t)}{\partial z^2} + m_s\frac{\partial^2 x(z,t)}{\partial t^2} = 0 \qquad (1)$$

where $x(z,t)$ is the transverse displacement of the beam, z and t are axial location and time respectively. EI is the bending stiffness. T_0 is the constant top tension, and T and ω_0 are the amplitude and frequency of fluctuating tension respectively. m_s is the structural mass per unit length. The solution of Eq. (1) is assumed as $x(z,t) = q_j(t)\sin j\pi z/l$, $j = 1, 2, 3, \ldots$ Then we have the Mathieu equation as follow:

$$\ddot{q}_j + {\omega_j}^2(1 - 2\theta\cos\omega_0 t)q_j = 0 \qquad (2a)$$

where

$$\omega_j = \left(\frac{j\pi}{l}\right)^2\left(\sqrt{\frac{EI}{m_s} + \frac{T_0 l^2}{(j\pi)^2 m_s}}\right), \quad j = 1, 2, 3, \ldots \qquad (2b)$$

is the natural frequency of the Euler beam with a constant tension T_0, and $\theta = T/2(T^* + T_0)$, $T^* = (j\pi/l)^2 EI$. If we set $q_1(t)$ and $q_2(t)$ as

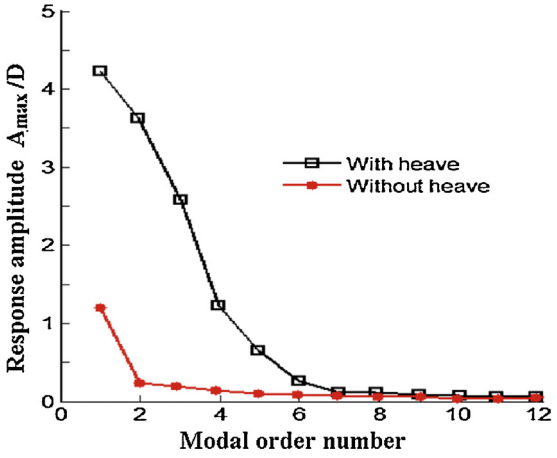

Fig. 4. Comparison of modal dynamic responses between the cases with top-end heave and without top-end heave.

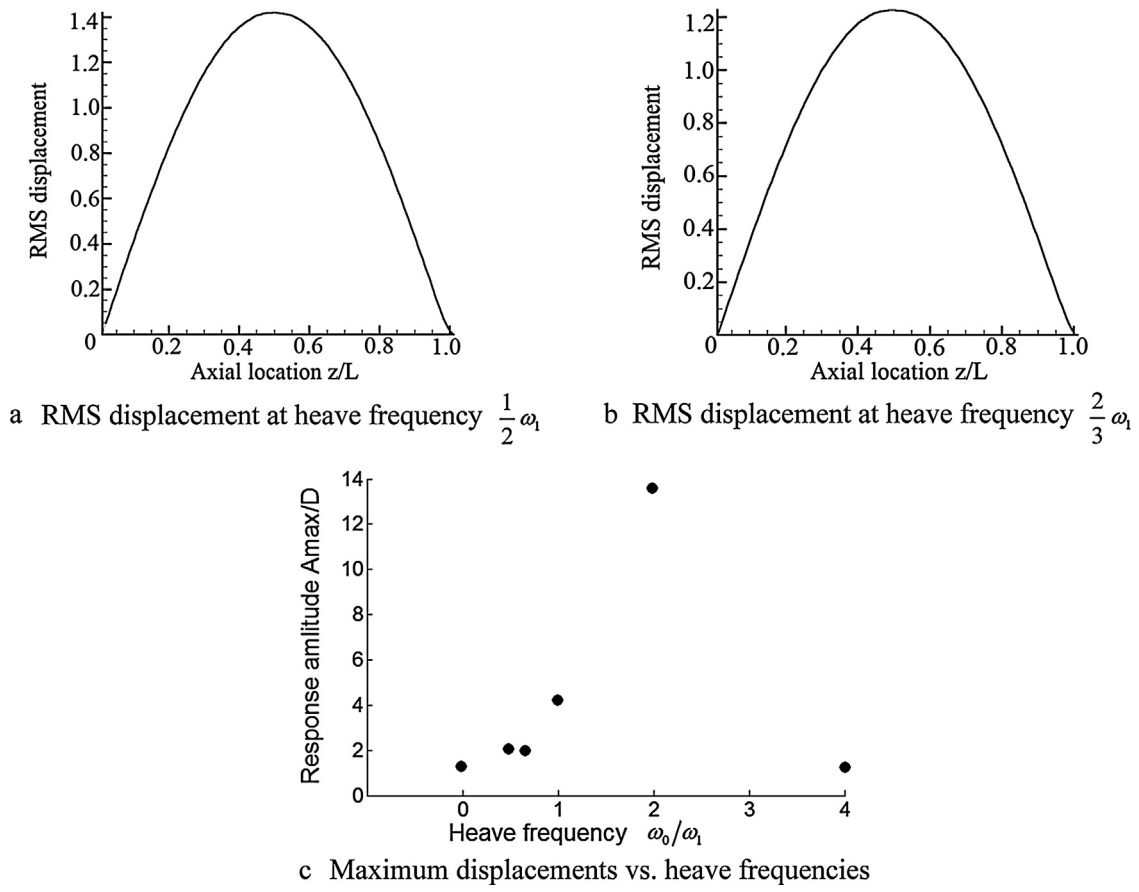

Fig. 5. Dynamic response of mode 1 at different top-end heave frequencies. (a) RMS displacement at heave frequency $1/2\omega_1$. (b) RMS displacement at heave frequency $2/3\omega_1$. (c) Max. displacement vs. heave frequency.

two particular solutions, with period t_0, of Eq. (2), then its eigen-equation can be written as

$$\lambda^2 - 2\lambda r + p = 0 \tag{3}$$

where $r = \frac{1}{2}[q_1(t_0) + \dot{q}_2(t_0)]$, $p = q_1(t_0)\dot{q}_2(t_0) - q_2(t_0)\ddot{q}_1(t_0)$.

To determine the stability boundary of the Mathieu equation, Eq. (2a), means to obtain the solution, with period t_0 or $2t_0$, of Eq. (3). When $|r| = 1$, and $\lambda_1 = \lambda_2 = \pm 1$, the periodic solutions of Eq. (3) are respectively as follows:

$$q(t) = d_0 + \sum_{k=2,4,6,\ldots}^{\infty} \left(c_k \cos\frac{k\omega_0 t}{2} + d_k \sin\frac{k\omega_0 t}{2} \right) \tag{4a}$$

$$q(t) = \sum_{k=1,3,5,\ldots}^{\infty} \left(c_k \cos\frac{k\omega_0 t}{2} + d_k \sin\frac{k\omega_0 t}{2} \right) \tag{4b}$$

Substituting Eqs. (4a) and (4b) into Eq. (3) yields:

$$\left(1 - \frac{\omega_0^2}{4\omega_j{}^2}\right)\left(1 - \frac{9\omega_0^2}{4\omega_j{}^2}\right)\left(1 - \frac{25\omega_0^2}{4\omega_j{}^2}\right)\ldots = 0 \tag{5a}$$

$$\left(1 - \frac{\omega_0^2}{\omega_j{}^2}\right)\left(1 - \frac{16\omega_0^2}{4\omega_j{}^2}\right)\left(1 - \frac{36\omega_0^2}{4\omega_j{}^2}\right)\ldots = 0 \tag{5b}$$

Combining above two equations, we have:

$$\omega_0 = \frac{2\omega_j}{k}, \quad k = 1, 2, 3\ldots \tag{6}$$

Eq. (6) indicates that a resonance may occur if excitation frequency ω_0 is related with natural frequency ω_j by Eq. (6), of which the response amplitude will approach infinite for a zero-damping system. Based on above stability analysis, though, that is done for an Euler beam, further researches [26,29] were generalized to other scenarios. Tang [26] classified all parametric resonances into three categories, i.e. the primary resonance if $\varpi = 1$ (the ratio of natural frequency to excitation frequency, $\varpi = \omega_i/\omega_0$), the sub-resonance if $\varpi = 1/n$ $(n = 2, 3, \ldots)$ and the super-resonance if $\varpi = n$ $(n = 2, 3, \ldots)$. Moreover, it is more complicated if two excitation frequencies of both top-end heave and vortex-induced lift force are involved. Wang [5] theoretically studied the case of an Euler beam undergoing top-end heave along with VIV. He found that a resonance may occur when three frequencies simultaneously satisfy $\omega_v \pm k\omega_0 = \omega_j$, $k = 0, 1, 2, 3\ldots$, where ω_v is vortex shedding frequency.

In practice, as for a platform system suffering both parametric excitation and VIV, its structural configuration is more complex rather than merely an Euler beam alone. Further, if the external loads regarding fluid-structure coupling or random distribution along riser span are considered, finite element simulation would a better option to analyze dynamic response of such a system. In this study, by developing an approach based on the FEM (finite element method) simulations, we will explore the impacts of top-end heave on the dynamic response of a coupling top-end & riser system.

2.2. Analytical model of dynamic response of integrate system

2.2.1. Structural model

The integrate system including both the top-vessel and riser is shown in Fig. 1. In Fig. 1a, the origin point of the coordinate system is located at the bottom end of the riser (fixed to the sea bed). The fluid flow, with velocity U, directs along the axis y. The heave motion of

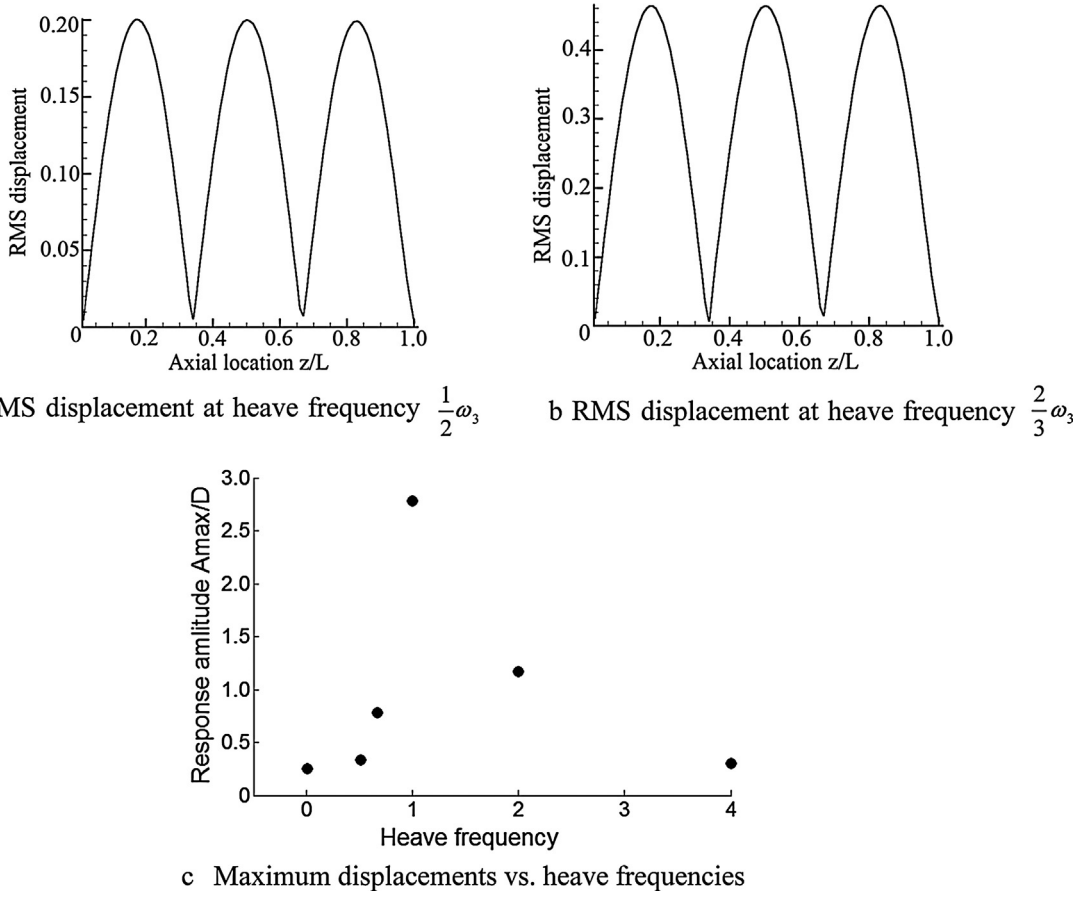

Fig. 6. Dynamic response of mode 3 at different top-end heave frequencies. (a) RMS displacement at heave frequency $1/2\omega_3$. (b) RMS displacement at heave frequency $2/3\omega_3$. (c) Max. displacement vs. heave frequency.

the top vessel is $b(t) = Be^{-i\omega_0 t}$, where B and ω_0 are respectively the amplitude and frequency. In the finite element model (shown in Fig. 1b), the top-end vessel and the riser respectively consist of 3D cubic solids and 1D Euler beam elements. The rotational motions around the axis x, y and z of all those grids of the top-end are constrained during the numerical simulations so as to avoid a probable singularity introduced by the extremely large mass of the top-end relative to the riser. Additionally, the multi-point constrain (MPC) is used at the joint grid connecting the top-end vessel and the riser, where different elements meet together, so that the constraints can be exerted effectively and smoothly upon different freedom degrees.

2.2.2. Hydrodynamic force model

The hydrodynamic force $F(z)$ consists of two parts, i.e. the vortex-induced lift force F_L and the fluid drag force F_D. The fluid drag force F_D can be expressed by the Morison's equation as

$$F_D = \frac{1}{2}C_D\rho_f D(U-\dot{x})\left|U-\dot{x}\right| + \frac{1}{4}C_a\pi D^2\rho_f(\dot{U}-\ddot{x}) + \frac{1}{4}\pi D^2\rho_f\dot{U}$$

where ρ_f is the fluid density. D is the riser outer diameter. C_D and C_a are the coefficients of the drag force and the added mass respectively, of which the values are $C_a = 1.0$ and $C_D = 1.1$ for a flexible riser with large aspect ratio.

When it comes to the vortex-induced lift force F_L, its expression becomes more complicated because VIV has always been a challenging issue concerning the interaction between fluid and structural dynamics. It is well known that riser's VIV exhibits some interesting, and even unexplained until now, traits like self-excitation, self-limitation of response amplitude, a variety of vortex-shedding modes, multi-mode or wide-band random vibration. Initially, vortex-induced lift force per unit length of a riser is written, somewhat similarly with the Morison's equation, as

$$F_L = \frac{1}{2}\rho_f U^2 C_L D$$

where the lift coefficient C_L is a constant value ranging from 0.5 to 1.2.

In recent years, with increasing amount of experimental observations in laboratories [2,30–32] and real fields along with CFD simulations, deeper understandings of VIV were reported. New approaches of lift force during lock-in were proposed, which are more accurate and reasonable because coupling between structural and fluid dynamics were taken into accounts [2,30,33]. Sarpkaya [1] experimentally measured the Fourier average of hydrodynamic force over many cycles of vibration. He decomposed the lift force into two parts, the drag part and the inertia part, which are respectively related to the velocity and acceleration of the vibrating cylinder. He pointed out that for practical Reynolds numbers, the nonlinear expression with respect to structural motion is able to capture the hydrodynamic feature better than the linear expression. Gopalfrishnan [30] and Govardhan [31] implemented plenty VIV experiments and presented the lift coefficient in terms of structural motion too. Vandiver [2] suggested that a piecewise parabola function of structural amplitude could be used for industrial model of lift force to calculate riser displacement by using wake oscillator model. Regarding above researches, we confidently think the lift coefficient C_L should depend on the structure motion rather than merely a constant value.

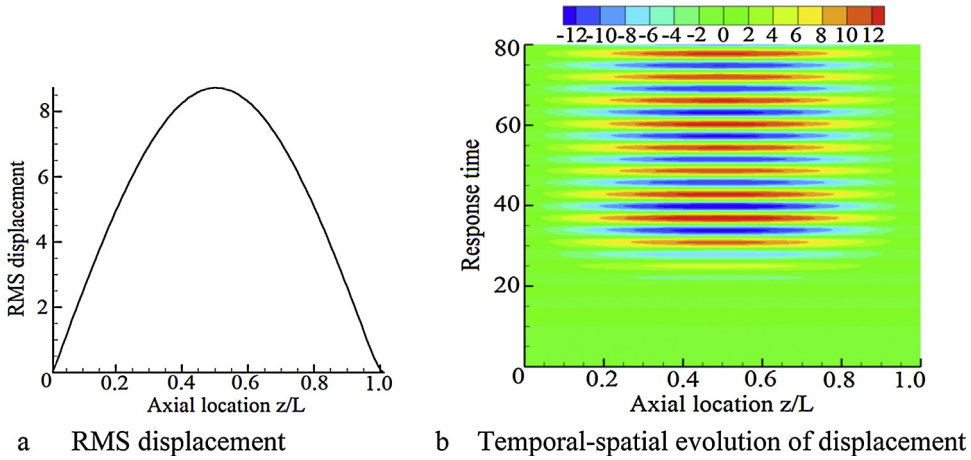

Fig. 7. Dynamic response at top-end heave frequencies, $\omega_0 = 2\omega_1$. (a) RMS displacement. (b) Temporal–spatial evolution of displacement.

Here, a third-order polynomial of the structure velocity is proposed to model the lift coefficient so as to take account of nonlinear interaction between structural and fluid dynamics, i.e.

$$F_L(x) = \frac{1}{2}\rho U^2 D(C_{L0}\sin(\omega t) + C_1\dot{x}(z,t) + C_2\dot{x}^2(z,t) + C_3\dot{x}^3(z,t)) = p_f C_L(\dot{x}(z,t)) \quad (7)$$

where $p_f = \frac{1}{2}\rho U^2 D$ and $C_L(\dot{y}(z,t)) = C_{L0}\sin(\omega t) + C_1\dot{x}(z,t) + C_2\dot{x}^2(z,t) + C_3\dot{x}^3(z,t)$ is the lift coefficient. The values of coefficients C_{L0}, C_1, C_2 and C_3 can be derived by fitting experimental data. Among those VIV experiments, the results based on the situations, such as a cylinder freely vibrating or flexible cable (with large aspect ratio) rather than forced vibration or rigid body, are strongly recommended, e.g. experiments of Gopalkrishnan [30] and Vandiver [2]. Chen [33] gave an approach to calculate the coefficients' values by fitting experimental data.

Observing Eq. (7), we may say it can capture, to some extents, features of VIV. (1) The feature of self-excitation. As we know, an action of exciting system to vibrate will happen as the reduced velocity falls into the lock-in range. In Eq. (7), this excitation is represented by the first term $p_f C_{L0}\sin(\omega t)$, a sinusoidal excitation force, together with the second term, $p_f C_1\dot{x}(z,t)$, which increases as response increases (C_1 is required to be positive). (2) The feature of self-limitation. One of unique traits of VIV is that structural response never rises infinitely, but begins to drop when its value reaches to a certain number, such as $\bar{y}_{\max} = 1.5$ or 2.0, in others words, the excitation for resonance becomes weaker while the damping is getting stronger. This feature, called self-limitation, is represented by the nonlinear terms with higher orders of structural motion in Eq. (7), $\rho_f C_2\dot{x}^2(z,t)$ or $\rho_f C_3\dot{x}^3(z,t)$ (at least one of the coefficients C_2 and C_3 is negative). (3) Axially varying distribution of lift force along riser's length. For case of a rigid cylinder, the vortex-induced lift force uniformly distributes along riser, and consequently the coherent length is equal to the length of the riser. But for case of a flexible slender riser, the coherence often reduces due to the non-uniform distributions of lift force as well structural motion. In the present model, the lift force is certainly non-uniform because of the axially varying amplitude of riser's response. Therefore, this model automatically captures the span coherence behavior of a flexible riser's VIV.

2.3. Model validation against experimental results

To validate the presented model, our numerical results are compared to experimental results (see Fig. 2), i.e. a rigid cylinder undergoing uniform flow by Khalak (1999) [34], the flexible cylinders respectively undergoing a uniform flow by Trim (2005) [35] and a sheared flow by Lie (2006) [36].

In the numerical simulations, the hydrodynamic coefficients are set to be $C_A = 1.0$, $C_d = 1.1$ which were determined based on the corresponding experiments [1]. Regarding the lift force of rigid cylinder is usually higher than that of flexible cylinder [1,2,31], we set the lift coefficients to be $C_{L0} = 0.50$, $C_{L1} = 1.82$, $C_{L2} = -1.29$, and $C_{L3} = -0.71$ for the rigid cylinder. And $C_{L0} = 0.22$, $C_{L1} = 1.62$, $C_{L2} = -2.31$ and $C_{L3} = +0.75$ for the flexible cylinders. Generally speaking, the calculated amplitudes have satisfied agreements with experimental results in different flow fields.

For the rigid cylinder, the experiment [34] indicated that there are three branches of response, i.e. the initial, upper and lower branches, through whole lock-in region. Here, the unsafest case, i.e. the upper branch where the corresponding reduced velocity V_r is 5.33, is considered. The time history of displacement is presented in Fig. 2a, where the experimental amplitude, as a compared one, is also plotted as a solid line (only the value of amplitude was presented in Ref. [34]). Fig. 2a shows that the calculated amplitude is slightly lower than the experimental value. The time history of displacement response, a harmonic sinusoid, implies that the response is characterized by single-mode vibration.

For the flexible cable in uniform flow [35], the numerical plot of the RMS displacement along riser length agrees with the experimental plot, see Fig. 2b. It also shows that the dominant mode is mode 3 and traveling wave is observed (no evident node is seen), that is consistent with the experimental result [35]. For the flexible cable in sheared flow (see Fig. 2c), the dominant mode of either the presented model or experiment is mode 11. And, the calculated displacement approximately agrees with the experimental displacement along most riser span, but somewhat differs from the experiment at the two ends of the riser. This difference may be caused by different types of dominating waves. Or, the calculated response is characterized mainly by a standing wave, while the experimental response exhibits an effect of traveling wave.

3. Effects of top-end vessel heave on riser's VIV

For a no-damping system, the amplitude of dynamic response would gradually rise up toward an infinite value if the system falls into instability region. For a practical system with a certain value of damping due to structural and fluid dynamics, the amplitude of dynamic response during parametric excitation would be a limited value which is larger than non-resonant cases. By cooperating the presented hydrodynamic model with the structure model, we carried out the dynamic response analysis of the integrate system

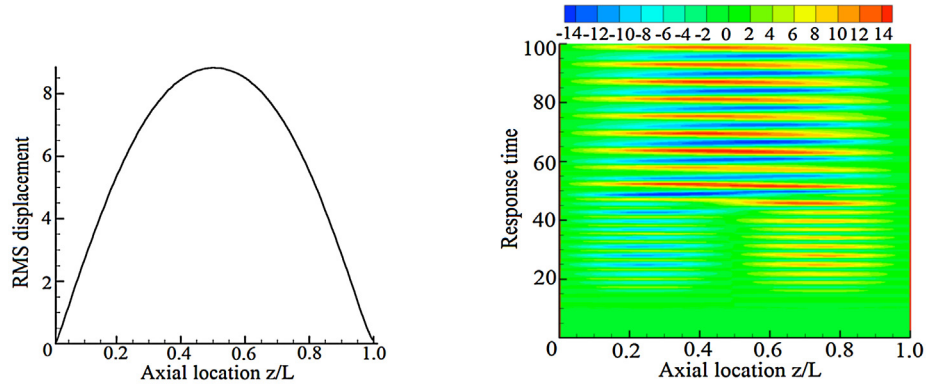

a RMS displacement b Temporal-spatial evolution of displacement

Fig. 8. Dynamic response at top-end heave frequencies, $\omega_0 = 2\omega_2$. (a) RMS displacement. (b) Temporal–spatial evolution of displacement.

(shown in Fig. 1) by using the FEM code (Chen et al., 2012). In order to explore the impacts of top-end vessel heave on riser's VIV, we will present the riser's displacement response and its wave propagation along riser length at different heave frequencies and tension ratios.

The structural parameters of the riser are as follows: the outer and inner diameters are respectively $D = 0.500$ m and $d = 0.445$ m. The riser length is 500 m, and the material density is $\rho_s = 7.8 \times 10^3$ (kg/m^3). The bending stiffness is $EI = 3.8 \times 10^9$ (Nm^2) and the structural damping ratio is 0.03. The top tension is $T = 6.8 \times 10^7$ (N) and the flow velocity is $U = 1.0$ m/s. The vortex-induced frequency is assumed consistent with the structural frequency, i.e. $\omega_v = \omega_j$.

3.1. Effect of heave frequencies on riser's dynamic response

3.1.1. At modal frequencies

The dynamic responses of the riser are numerically simulated while the top-end is heaving at the riser's natural frequencies of modes ranging from mode 1 to mode 24, and the frequency of vortex-induced lift force is the same as the heave frequency. Selected displacements of the dynamic response are presented in Fig. 3. Generally speaking, the response displacements increase as the heave frequencies decreases. It is also noted that the modal responses of lower-order modes are mostly dominated by standing wave, while the traveling wave can been obvioinusely seen in the responses of higher-order modes, see Fig. 3e and f where there is no longer exact node. This is mainly because the dynamic modal response of the mode with higher order number attanuates faster than lower modes. Thus, the riser's vibration attenuates rapidly to small value, even zero, before it meets the reflect wave to form a standing wave. Also, as modal order number inceases, structural deformation curvature gets larger. Thus, compared with the tesion stiffness, the bending stifness becomes more significant, in other words, the effect of dynamic tension on displacement response gets smaller.

The comparison of the maximum amplitudes between the cases with top-end heave and without top-end heave is presented in Fig. 4. It is shown that the maximum amplitudes of the riser experiencing both top-end heave and VIV are larger than the cases without top-end motion. Take mode 1 as an example, its maximum amplitude is about twice larger than the case without top-end heave.

Moreover, if observing the displacement responses of the riser undergoing both VIV and top-end heave, i.e. Figs. 3a and 4, we note that the value of the displacement sometimes is larger than that of VIV alone (1.5 for VIV) or, even, that of parametic excitation alone. That is partly because the nonlinear interaction between top-end motion (along with, consequently, the axial motion) and the riser's VIV, which might nonlineally amplify the dynamic response of the riser. The phenonmina, a combination of vertical and lateral excitation giving greater amplitude, were also reported in Refs. [7,29,37].

Table 1
Riser's natural frequencies unit: Hz.

Mode number	1	2	4
Frequency/Hz	0.1715	0.3415	0.6917

3.1.2. At other frequencies

For the case of top-end heaving at other frequencies, different from the modal frequencies such as $\omega_0 = \omega_j, 1/2\omega_j, 2/3\omega_j, 2\omega_j, 4\omega_j$, the dynamics responses are presented in Fig. 5. Comparing Fig. 5a and b where the heave frequencies are respectively $\omega_0 = 1/2\omega_1$ and $\omega_0 = 2/3\omega_1$, we note that the dynamic response amplitudes change at different heave frequencies but the modal shapes of RMS displacement almost do not change. Fig. 5c indicates that three largest amplitudes of dynamic response are respectively at the heave frequencies $\varpi = 1$, $1/2$ and 2 Particularly, the largest response amplitude occurs at frequency $\varpi = 2$. Or, we may say, for mode 1, the largest dynamic response might occur when top-end heave frequency is twice as much as the natural frequency, i.e. $\omega_0 = 2\omega_1$.

But for mode 3, the dynamics responses, see Fig. 6, is somewhat different from mode 1. In Fig. 6c, the largest response amplitude is at the frequency $\varpi = 1$, but not as it is in Fig. 5c.

An interesting phenomenon, called "mode transition" here, is observed during the dynamics responses at some special frequencies, which, we think, might be a consequence of frequency multiplication owing to the natural dynamics characteristics of the riser. Similar phenomenon (called "mode jump" there) is reported by Silveira [6] who used Hilbert–Huang spectral analysis technique helps distinguishing mode jumps by tracking frequency responses in time. Park [7] also pointed out that the parametric excitation may alter the response pattern of a long slender marine structure.

We think the frequency multiplication of the riser, due to its natural dynamics characteristics, is mainly responsible for the mode transition in our numerical simulations. According to Eq. (2b), for the modes with lower modal order number, the value of natural frequency is approximately proportional to the order number, j, because the tension stiffness is much larger than the bending stiffness. In that case, there does exist frequency multiplications. The natural frequencies of the riser are listed in Table 1, where we can see that $\omega_2 \approx 2\omega_1$, $\omega_4 \approx 2\omega_2$.

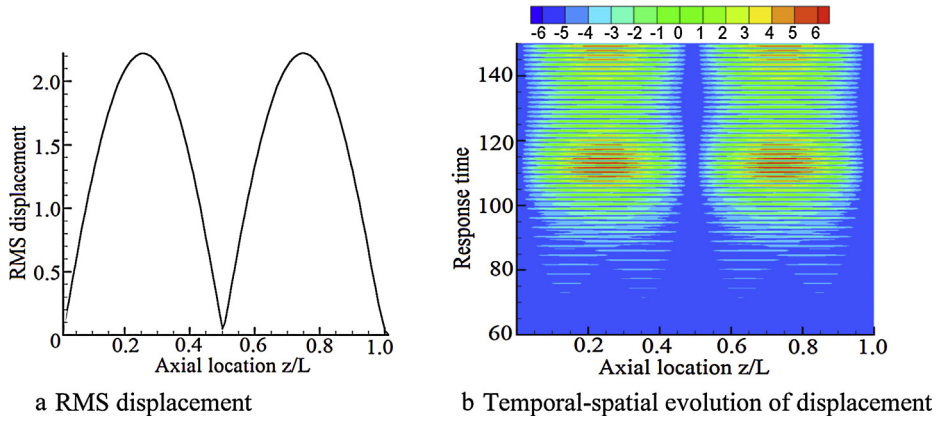

Fig. 9. Dynamic response at top-end heave frequencies, $\omega_0 = 2\omega_4$. (a) RMS displacement. (b) Temporal–spatial evolution of displacement.

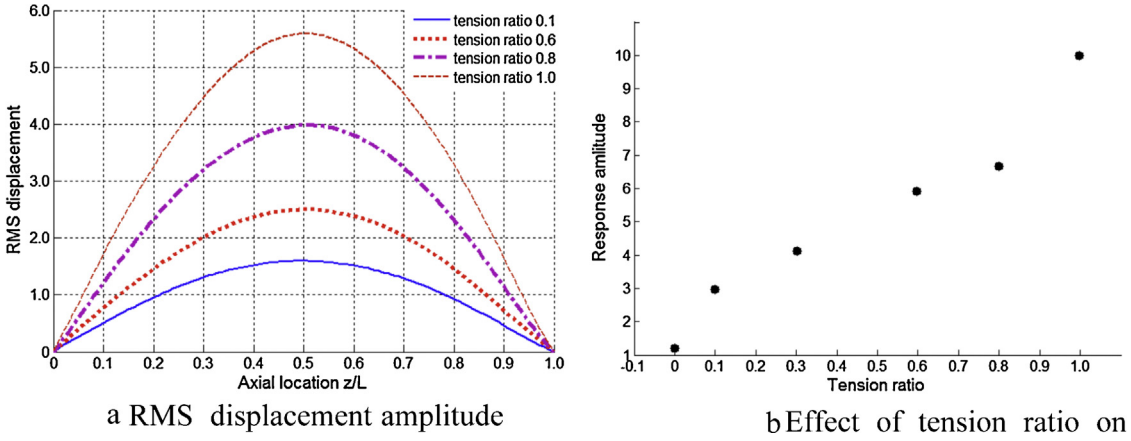

Fig. 10. Riser's dynamics responses of mode 1 at different tension ratios. (a) RMS displacement. (b) Effect of tension ratio on amplitude.

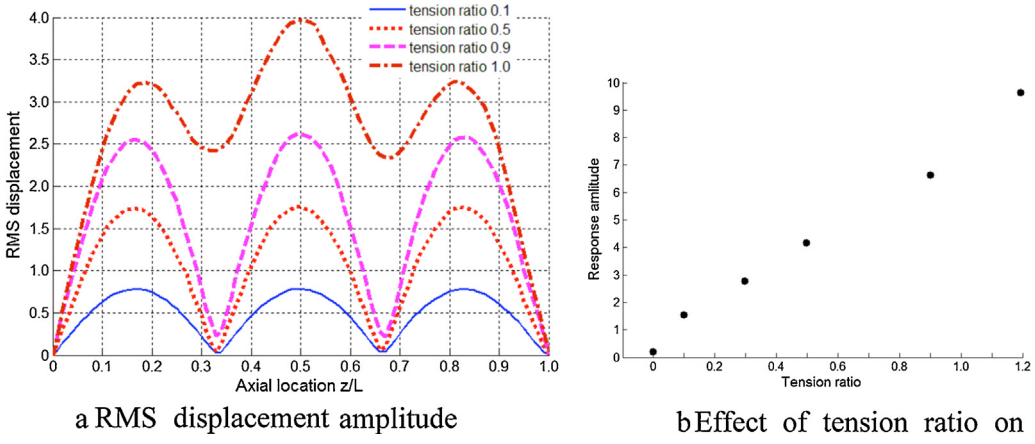

Fig. 11. Riser's dynamics responses of mode 3 at different tension ratios. (a) RMS displacement. (b) Effect of tension ratio on amplitude.

For cases of the excitation frequencies being $\omega_0 = 2\omega_1$, $\omega_0 = \omega_2$ and $\omega_0 = \omega_4$, the dynamic responses in terms of RMS displacement and temporal-spatial evolution are present in Figs. 7–9 respectively. Comparing Figs. 7a and 8a, we can see that the two plots of the RMS displacements look quite alike and have almost same displacement values. But if observing the temporal-spatial evolutions of displacement, see Fig. 7b and 8b, we can see an interesting difference. As $\omega_0 = \omega_2$, see Fig. 8b, the displacement wave shifts from the modal shape of mode 2 to mode 1, called mode transition, after a period of dynamic response. Moreover, the displacement becomes larger after the mode transition happens. This phenomenon is also observed for case of the excitation $\omega_4 \approx 2\omega_2$, that the response displacement wave shifts from mode 4 to mode 2 meanwhile the displacement becomes larger, see Fig. 9b.

3.2. *Effect of tension ratio*

Effect of the amplitude of fluctuating tension on riser's dynamic response is examined for different modes. Selected results, of mode 1 and mode 3, are respectively presented in Figs. 10 and 11 where the tension ratio $\bar{T} = T/T_0$ is the ratio of the amplitude of the fluctuating tension to the constant tension. It is seen, in both

Figs. 10 and 11, that the response displacements get larger as the tension ratio rises from 0.1 to 1.0. And, the largest amplitude rises almost lineally with the increase of tension ratio. It is also noted that the dynamic response is mostly dominated by standing wave. But with the tension ratio increasing, the dynamics response might be characterized by traveling wave, e.g. as $\bar{T} = 1.0$ show in Fig. 11a.

4. Conclusions

The dynamic responses of the integrate system including both a moving top-end and a riser undergoing VIV are examined by means of finite element simulations. It is shown that the displacement amplitudes of the riser experiencing both top-end heave and VIV are larger than that without top-end motion. And, a combining excitation of top-end heave and lateral VIV may give greater displacement of the riser's dynamic response than that of VIV alone or, even, that of parametic excitation alone. We suggest that, in practices of riser design, a combined excitation needs to be considered for the accurate dynamic analysis of slender marine structures subjected to a top-end motion and VIV. Our numerical results show following conclusions:

(1) The riser's displacement gets more pronounced as the number of modal order drops. The dynamics responses of the modes with lower order number are mostly dominated by standing wave, while traveling wave can be seen in the responses of the modes with higher order number.
(2) Mode transition is observed at some particular excitation frequencies, being twice of natural frequency, during riser's dynamic response owing to the frequency multiplication of the riser's dynamic characteristics.
(3) The response displacement gets larger as the tension ratio rises. And, the largest amplitude almost lineally rises with the increase of tension ratio.

Acknowledgment

The authors of this paper would like to thank the financial support provided by the National Natural Sciences Foundation (Grant Nos. 11232012 and 11372320).

References

[1] Sarpkaya T. A critical review of the intrinsic nature of vortex-induced vibration. J Fluids Struct Mech 2004;46:389–447.
[2] Vandiver JK. A universal reduced damping parameter for prediction of vortex-induced vibration. In: Proceedings of the ASME 21st International Conference on Ocean, Offshore and Arctic Engineering OMAE2002. 2002.
[3] Stansberg CT, Ormberg H, Oritsl O. Challenges in deep water experiments: hybrid approach. J Offshore Mech Arctic Eng 2002;124:91–6.
[4] Garrett DL. Coupled analysis of floating production systems. Ocean Eng 2005;32:802–16.
[5] Wang DY, Ling GC. Vortex-induced nonlinear vibration of TLP tethers under circumstances of platform oscillation. Acta Oceannol Sin 1998;20(5):119–28 [in Chinese].
[6] da Silveira LMY, Martins CdA, Leandro DC, Pescee CP. An investigation on the effect of tension variation on VIV of risers. In: Proceedings of the ASME 20th International Conference on Ocean, Offshore and Arctic Engineering OMAE2007-29247. 2007.
[7] Park HI, Jung DH. A finite element method for dynamic analysis of long slender marine structures under combined parametric and forcing excitations. Ocean Eng 2002;29:1313–25.
[8] Ormberg H, Fylling IJ, Larsen K, Sodahl N. Coupled analysis of vessel motions and mooring and riser system dynamics. In: Proceedings of the ASME 16th International Conference on Ocean, Offshore and Arctic Engineering OMAE1997. 1997.
[9] Kim MH, Arcandra T, Kim YB. Variability of spar motion analysis against various design methodologies/parameters. In: Proceedings of the ASME 20th International Conference on Ocean, Offshore and Arctic Engineering OMAE2001. 2001.
[10] Spanos PD, Ghosh R, Finn LD. Coupled analysis of a spar structure: Monte Carlo and statistical linearization solutions. J Offshore Mech Arctic Eng 2005;127(1):11–6.
[11] Wichers JEW, Voogt HJ, Roelofs HW, Driessen PCM. DeepStar-CTR 4401 Benchmark Model Test. Technical Report No. 16417-1-OB, MARIN, Netherlands; 2001.
[12] Bosman RLM, Hooker J. Elastic modulus characteristics of polyester mooring ropes. Proc Annu Offshore Technol Conf 1999;124:6–1251.
[13] Heurtier JM, Buhan L, Fontaine E. Coupled dynamic response of moored FPSO with risers. Proc Eleventh Int Offshore Pol Eng Conf 2001:17–22.
[14] Chen XH, Ding Y, Zhang Y. Coupled dynamic analysis of a mini TLP: comparison with measurements. Ocean Eng 2006;33:93–117.
[15] Gu JY, Lu HN, Yang JM. Studies on coupling dynamic response and characteristics mooring system of TLP in stochastic waves. Ocean Eng 2012;30(4):42–8 [in Chinese].
[16] Li BB, Ou JP, Teng B. Fully coupled effects of hull: mooring and risers model in time domain based on an innovative deep draft multi-spar. Chin Ocean Eng 2010;24(2):219–33.
[17] Tahara A, Kim MH. Hull/mooring/riser coupled dynamic analysis and sensitivity study of a tanker-based FPSO. Appl Ocean Res 2003;25:367–82.
[18] Lee HH, Wang PW. Analytical solution on the surge motion of tension-leg twin platform structural systems. Ocean Eng 2000;27:393–415.
[19] Tahara A, Kim MH. Coupled-dynamic analysis of floating structures with polyester mooring lines. Ocean Eng 2008;35(17–18):1676–85.
[20] Tang YG, Shao WD, Zhang J, et al. Dynamic response analysis for coupled parametric vibration and vortex-induced vibration of top-tensioned rise in deep-sea. Eng Mech 2013;5:282–6 [in Chinese].
[21] Patel MH, Park HI. Dynamics of tension leg platform tethers at low tension. Part I – Mathieu stability at large parameters. Mar Struct 1991;4:257–73.
[22] Chatjigeorgiou IK. On the parametric excitation of vertical elastic slender structures and the effect of damping in marine applications. Appl Ocean Res 2004;26:23–33.
[23] Chandrasekaran S, Chandak NR, Anupam G. Stability analysis of TLP tethers. Ocean Eng 2006;33:471–82.
[24] Simos AN, Pesce CP. Mathieu stability in the dynamics of TLP's tethers considering variable tension along the length. Trans Built Environ 1997;29:41–8.
[25] Han SM, Benaroya H. Non-linear coupled transverse and axial vibration of a compliant structure, part 2: forced vibration. J Sound Vib 2000;237(5):875–900.
[26] Tang JS, He XZ. Response analysis of parametrically excited system. J Yueyang Norm Univ (Nat Sci) 2001;14(1):34–40 [in Chinese].
[27] Yang HZ, Xiao F. Instability analyses of a top-tensioned riser under combined vortex and multi-frequency parametric excitations. Ocean Eng 2014;81(0):12–28.
[28] Jian YJ, XQ E, Bai W. Nonlinear faraday waves in a parametrically excited circular cylindrical container. Appl Math Mech 2003;24(10):60–6.
[29] Xu WH, Zeng XH, Wu YX. Hill instability analysis of TLP tether subjected to combined platform surge and heave motions. Chin Ocean Eng 2008;22(4):533–46.
[30] Gopalkrishnan R [Ph.D.Thesis] Vortex induced forces on oscillating bluff cylinders. MA, USA: MIT, Cambridge; 1993.
[31] Govardhan R, Williamson CHK. Critical mass in vortex-induced vibration of a cylinder. Eur J Mech B/Fluids 2004;23:17–27.
[32] Sanaati B, Kato N. A study on the effects of axial stiffness and pre-tension on VIV dynamics of a flexible cylinder in uniform cross-flow. Appl Ocean Res 2012;37(0):198–210.
[33] Chen WM, Li M, Zheng ZQ. Dynamic characteristics and VIV of deepwater riser with axially varying structural properties. Ocean Eng 2012;42:7–12.
[34] Khalak A, Williamson CHK. Motions, forces and mode transitions in vortex-induced vibrations at low mass-damping. J Fluids Struct 1999;13:813–51.
[35] Trim AD, Braaten H, Lie H. Experimental investigation of vortex-induced vibration of long marine risers. J Fluids Struct 2005;21:335–61.
[36] Lie H, Kaasen HK. Model analysis of measurements from a large-scale VIV model test of a riser in linearly sheared flow. J Fluid Struct 2006;22:557–75.
[37] Patel MH, Park HI. Combined axial and lateral responses of tensioned buoyant platform tethers. Eng Struct 1995;17(10):687–95.